NM16072201: accepted manuscript

Phagocytosis-inspired behaviour in synthetic protocell communities of compartmentalized colloidal objects

Laura Rodríguez-Arco, Mei Li and Stephen Mann*

Centre for Protolife Research and Centre for Organized Matter Chemistry, School of Chemistry, University of Bristol, Bristol BS8 1TS, United Kingdom.
*email: laura.rodriguezarco@bristol.ac.uk, mei.li@bristol.ac.uk, s.mann@bristol.ac.uk

The spontaneous assembly of micro-compartmentalized colloidal objects capable of controlled interactions offers a step towards rudimentary forms of collective behaviour in communities of artificial cell-like entities (synthetic protocells). Here we report a primitive form of artificial phagocytosis in a binary community of synthetic protocells in which multiple silica colloidosomes are selectively ingested by self-propelled magnetic Pickering emulsion (MPE) droplets comprising particle-free fatty acid-stabilized apertures. Engulfment of the colloidosomes enables selective delivery and release of water-soluble payloads, and can be coupled to enzyme activity within the MPE droplets. Our results highlight opportunities for the development of new materials based on consortia of colloidal objects, and provide a novel microscale engineering approach to inducing higher-order behaviour in mixed populations of synthetic protocells.

The spontaneous self-assembly and integration of molecular and nanoscale building blocks into semi-permeable aqueous micro-compartments offer new approaches to the design and construction of rudimentary artificial cell-like constructs (protocells) with biomimetic functions.[1,2] Such micro-ensembles could have relevance in the aqueous sequestration and clean-up of trace pollutants, targeted drug storage and delivery, control of microscale chemical reactions, and origins of life research.[3-5] Recently, we developed an artificial protocell model derived from the spontaneous assembly of partially hydrophobic silica nanoparticles at the water droplet/oil interface.[6-8] Biomolecules such as genetic polymers and enzymes were encapsulated into the nanoparticle-stabilized aqueous droplets (water-in-oil Pickering emulsions[9-12]), and the silica membrane was cross-linked in oil to produce colloidosomes in the form of robust, semi-permeable microcapsules that could be transferred into water.[6] A range of protocellular functions were subsequently demonstrated, including *in situ* gene expression,[6] enzyme-mediated catalysis,[6,8,13] microcapsule growth and division,[7] membrane gating,[8] enzyme-directed secretion of an extracellular-like matrix,[14] and enzyme-induced small-molecule signalling.[15]

The above studies, along with diverse investigations on alternative protocell models,[16-24] have focused primarily on the integration of functional components into individual micro-compartmentalized constructs. In contrast, the collective and dynamic behaviour of synthetic protocell populations has received relatively little attention even though materials based on consortia of micro-compartmentalized colloidal objects could have potential use in synergistic sensing systems and biomimetic systems engineering.[25] Recently, an artificial form of predatory behaviour in an interacting community of protease-containing coacervate micro-droplets and

protein-polymer microcapsules (proteinosomes) has been demonstrated.[26] In this paper, we address the challenge of how to design micro-compartmentalized colloidal objects as a model of a synthetic protocell community exhibiting a rudimentary form of artificial phagocytosis based on controlled engulfment (Fig. 1). The process is established in dodecane containing a size-mismatched binary population of iron oxide (magnetite, Fe_3O_4) particle-stabilized water-in-oil magnetic Pickering emulsion (MPE) droplets and targeted cross-linked aqueous-filled silica colloidosomes. Specifically, we show that oleic acid-induced changes in interfacial tension produce self-propelled or magnetically guided MPE droplets comprising localized particle-free fatty acid-stabilized apertures through which ingestion of multiple intact silica colloidosomes occurs. We demonstrate that the engulfed colloidosomes can deliver and release a water-soluble payload to trigger an enzyme reaction inside the host MPE droplets. Overall, our results constitute a first step towards the design and engineering of a synthetic protocell community capable of a primitive form of phagocytosis-inspired behaviour, and offer an approach to new materials with higher-order function and behaviour that arise in mixed populations of micro-compartmentalized colloidal objects.

Aperture formation in MPE droplets

Magnetically responsive water-in-oil Pickering emulsion droplets (Fig. 2a) were prepared by spontaneous interfacial assembly of partially hydrophobic magnetic particles (mean diameter = 500 ± 180 nm, Supplementary Fig. 1) dispersed in a mixture of water and dodecane. The MPE droplets consisted of a continuous spherical shell of closely packed oleate-capped magnetite (Fe_3O_4) particles, were structurally stable at room temperature over several weeks, and exhibited mean diameters (typically 500 ± 250 μm) that were dependent on the magnetite weight/water volume ratio (Supplementary Fig. 2). Consistent with other studies on emulsion-based protocell models,[6-8,15,27,28] a range of synthetic and biological molecules, such as fluorescent-tagged polysaccharides and proteins could be encapsulated into the MPE droplets (Fig. 2b,c). Application of an external magnetic field had negligible influence on the structure of the magnetite shell, which remained closely packed and free of macropores. Optical microscopy images showed chain-like arrays of MPE droplets aligned parallel to the magnetic field direction, indicating that linear arrays of the micro-compartmentalized objects could be readily organized using a neodymium magnet (Fig. 2d).

We exploited the surfactant-mediated partial destabilization and redistribution of the iron oxide shell of MPE droplets prepared at pH 10.2 (0.1 M carbonate buffer) as a strategy to induce controlled opening of the inorganic membrane. Addition of oleic acid to the oil phase of a MPE droplet suspension at a concentration ≤ 1 mg mL^{-1} increased the fluidity of the magnetic membrane such that magnetite-free apertures appeared within the inorganic shell of the MPE droplets (Fig. 2e,f). Increasing the oleic acid concentration above 1 mg mL^{-1} produced more complex colloidal objects (Fig. 2g,h), which often exhibited a Janus-like structure comprising a static high-density magnetic particle domain in association with a fluid particle-free interface in the form of irregular apertures delineated by a distinct boundary of loosely packed magnetite particles (Fig. 2i). The surface area occupied by the particle-free domains showed an estimated

increase from *ca.* 15 to 40% as the oleic acid concentration was raised from 0.25 to 2 mg mL^{-1} (Fig. 2j). Similar experiments on MPE droplets prepared at pH values below the apparent pK_a of oleic acid (9.84) indicated that aperture formation was progressively inhibited (Fig. 2j). We therefore attributed restructuring of the magnetite membrane to a pH-dependent decrease in interfacial tension associated with the adsorption of negatively charged oleate molecules at the oil/water interface (Supplementary Fig. 3), which resulted in partial displacement of the inorganic particles and formation of fatty acid-stabilized patches (Supplementary Note).

Phagocytosis-inspired engulfment of colloidosomes

We exploited the oleate-induced opening of the MPE droplets and decrease of the oil/water interfacial tension to induce a rudimentary form of artificial phagocytosis in binary populations of size-mismatched MPE droplets (pH 10.2) and target cross-linked silica colloidosomes dispersed in oleic acid-containing dodecane. The aqueous-filled (pH ≈ 6.2) colloidosomes were typically 5 to 25 times smaller (mean size = 50 ± 20 μm) than the MPE droplets, such that single MPE droplets ingested multiple colloidosomes. We introduced a limited number of MPE droplets (typically one or two) into the silica colloidosome suspension to minimize deleterious MPE-MPE fusion events through the oleate domains, and investigated the mixtures immediately by optical and fluorescence microscopy. In the absence of oleic acid, the MPE droplets and silica colloidosomes remained separate and non-interacting. Engulfment of the silica colloidosomes by the MPE droplets was also negligible at low concentrations of oleic acid (≤ 1 mg mL^{-1}) even though around 20% of the droplet area was associated with the fatty acid-stabilized apertures (Fig. 2j). However, remote manipulation of the MPE droplets into direct contact with the silica colloidosomes using an externally hand-held magnet along with magnetically induced redistribution of the iron oxide particles near to the attached colloidosomes gave rise to slow penetration of the silica colloidosomes through newly formed entry points in the MPE droplet membrane (Supplementary Movie 1 and Fig. 3a). Whilst engulfment of the intact colloidosomes could be achieved without contact with the underlying substrate (Supplementary Movie 1), *in situ* formation of the fatty acid-stabilized patches also increased the localized wetting behaviour of the MPE droplets on the polystyrene surface such that neighbouring silica colloidosomes were spontaneously ingested in the presence of the magnetic field (Supplementary Movie 2). Removal of the magnetic field re-established a more isotropic particle distribution in the magnetite shell and therefore switched off the artificial phagocytosis behaviour (Supplementary Movie 2).

The above dynamical behaviour became more prevalent as the oleic acid concentration was increased to 2 mg mL^{-1} for MPE droplets prepared at pH = 10.2. Under these conditions, both the surface area associated with the exposed particle-free entry points as well as the extent of localized wetting at the periphery of the MPE droplets were increased. As a consequence, individual MPE droplets spontaneously ingested numerous silica colloidosomes located in their near proximity even in the absence of a magnetic field. Penetration of intact silica colloidosomes into the MPE droplets occurred specifically at the particle-free regions, with transit times through the fatty acid-stabilized interface of a few seconds (Fig. 3b). As a

consequence, up to ~8% of the colloidosomes observed in the field of view of the optical microscope were engulfed by the MPE droplets within a period of 60 s (Fig. 3c and Supplementary Fig. 4). Using a magnetic field to guide the MPE droplets specifically towards the silica colloidosomes approximately doubled the number of ingested colloidosomes (Supplementary Fig. 4).

Engulfment of the silica colloidosomes by the MPE droplets was associated with spontaneous lateral movement of some of the individual droplets (Supplementary Movie 3), and high turbulence within their interior (Supplementary Movie 4). Self-propulsion of the droplets was attributed to instabilities associated with Marangoni convective flow[29] along the droplet interface under non-equilibrium conditions, and produced a series of short-distance displacements and rotations that facilitated contact with the surrounded colloidosomes. The turbulence exhibited a quasi-bilateral flow pattern that was characteristic of the Marangoni effect[29] (Supplementary Movie 5), and was attributed to the formation of a gradient in interfacial tension due to a heterogeneous distribution of oleate/oleic acid molecules at the surface of the MPE droplets. Specifically, deprotonation-induced transfer of oleic acid through the dodecane/water interface leads to a local variation of the interfacial tension, which in turn generates a Marangoni surface stress towards the regions with higher surface tension. Counter-balancing of the surface and viscous stresses result in tangential forces and the dragging of the adjacent fluid layers on both sides of the interface to produce Marangoni flows from the low to high regions of interfacial tension.[29,30] Significantly, when the gradient in interfacial tension is directed towards one side of the droplets then the emerging flow pattern gives rise to self-propulsion in a direction opposite to the Marangoni flows. Compared with previous reports on self-propelled oil droplets in water that exhibit sustained motion in diverse directions due to chemical charging at the interface,[30-32] the MPE droplets were intermittently active for a few seconds only and limited in their range of displacement, suggesting that the gradients in interfacial tension were readily dissipated. Interestingly, the MPE droplets moved only with the oleate-stabilized aperture as the leading edge, indicating that the segregated magnetite and oleate domains were associated with regions of low and high interfacial tension, respectively.

We undertook a series of experiments to confirm that decreases in interfacial tension associated with the adsorption of oleate anions at the MPE droplet surface were responsible for aperture formation and the onset of the phagocytosis-like behaviour. Increasing the oleic acid concentration to 2 mg mL^{-1} increased the percentage of colloidosomes engulfed at pH 10.2 in the absence of a magnetic field, and reducing the pH to 8.3 or 5.5 effectively curtailed this activity (Fig. 3c). Moreover, the engulfment efficiency of MPE droplets prepared at pH 10.2 and oleic acid concentration of 2 mg mL^{-1} was decreased when aqueous solutions with increased oil/water interfacial tension values ($\gamma_{o/w}$) were encapsulated within the silica colloidosomes (Supplementary Fig. 4). For example, the rate of ingestion of colloidosomes containing aqueous 0.1 M NaCl ($\gamma_{o/w}$ = 49 ± 2 mN m^{-1}) was very slow (Supplementary Movie S6), whilst those containing polyalcohols such as carmine/curcumine dispersed in a mixture of glycerol and water ($\gamma_{o/w}$ = 6.1 ± 1.5 mN m^{-1}) were engulfed rapidly depending on the concentration of the entrapped solutions (Supplementary Fig. 4). Control experiments indicated that the percentage

of oleic acid transferred from oil to water increased from < 20 % for pH values lower than the pK_a (9.84) of oleic acid to ≈ 100 % at pH 12 (Supplementary Fig. S5), and showed that the aqueous concentrations of oleate used in the experiments at pH 10.2 were considerably higher than the critical micelle concentration (0.012 mg mL^{-1} at pH 10). It therefore seems most probable that the silica colloidosomes are coated in an oleate monolayer prior to engulfment, and that translocation of the intact colloidosomes through the oleate-stabilized apertures is facilitated by *in situ* formation of a hydrophilic fatty acid bilayer or multilayer on the colloidosome external surface (Fig. 3d).

Engulfment-mediated transfer of payloads

Phagocytosis-inspired intake of the colloidosomes was associated with the selective delivery and release of water-soluble chemicals into the MPE droplets. Proteins such as FITC-labelled bovine serum albumin (FITC-BSA) were retained within the engulfed colloidosomes (Fig. 4a,b), whilst small molecules such as calcein (Fig. 4c,d) or carmine (Fig. 4e) were released through the semi-permeable silica membrane into the water phase of the MPE droplets. To deliver colloidosome-entrapped macromolecules into the aqueous interior of the MPE droplets we employed non-crosslinked colloidosomes (i.e. silica-stabilized Pickering emulsion droplets) as the target objects for engulfment. In such cases, disassembly of the silica shell occurred spontaneously on transfer into the MPE interior to release payloads such as fluorescent proteins and micron-sized polystyrene beads (Supplementary Movie 7). We utilised the above observations to undertake phagocytosis-like transfer and delivery of reagents for initiating spatially confined reactions inside the MPE droplets (Fig. 4f,g). As a proof of concept, we encapsulated alkaline phosphatase (ALP) (1650 units mL^{-1}) within the MPE droplets and prepared silica colloidosomes containing the non-fluorescent small-molecule substrate fluorescein diphosphate, and used fluorescence microscopy and bright field imaging to monitor the coupling of engulfment with ALP-mediated dephosphorylation and formation of the green fluorescent product fluorescein. Optical fluorescence microscopy video images showed that green fluorescence in the MPE droplets was triggered by ingestion of the colloidosomes and release of fluorescein diphosphate through the pores of the cross-linked silica membrane (Supplementary Movie 8). Whilst contact with the iron oxide shell of the MPE droplet did not give rise to green fluorescence, the enzyme reaction was immediately activated when the colloidosomes were transferred across the magnetite-free open regions (Fig. 4h). Fluorescence was observed initially in close proximity to each ingested colloidosome and then became quickly dispersed throughout the MPE droplet by the Marangoni-induced turbulence. Time-dependent measurements of fluorescence intensity on single MPE droplets undergoing episodic engulfment of individual fluorescein diphosphate-containing colloidosomes showed that the green fluorescence increased within 1-2 s after ingestion to a maximum value that was approximately proportional to the volume of the ingested colloidosome (Fig. 4i and Supplementary Movie 9). This was followed by a slow decrease in fluorescence intensity due to dilution of the fluorescein product by turbulence inside the MPE droplet. Subsequent episodic engulfment of other colloidosomes produced a series of pulses in localized fluorescence

intensity. Overall, these results demonstrate the feasibility of stepwise delivery of reagents between micro-compartmentalized colloidal objects, and constitute a first approach towards the induction of multiple reactions within communities of model synthetic protocells.

Conclusions

In conclusion, surfactant-mediated partial destabilization and redistribution of the iron oxide shell of MPE droplets has been employed as a strategy to induce phagocytosis-like behaviour in a size-mismatched binary community of micro-compartmentalized colloidal objects dispersed in dodecane. Adsorption of sufficient amounts of oleate molecules at the water/oil interface reduces the interfacial tension and produces self-propelled MPE droplets comprising internalized Marangoni instabilities and particle-free apertures, which serve as entry points for the ingestion of intact cross-linked silica colloidosomes and their various payloads. In contrast, low concentrations of the fatty acid require remote manipulation of the magnetic particles in the MPE droplet membrane to open the magnetite shell for colloidosome ingestion. Colloidosome penetration is also dependent on establishing an alkaline pH in the MPE droplets, and can be further enhanced by the presence of surface-active solutes entrapped within the colloidosomes, and by remote guidance of the individual MPE droplets using an external magnetic field. As engulfment of the colloidosomes is associated with the delivery and release of water-soluble chemicals, phagocytosis-inspired behaviour can be coupled to the triggering of enzyme activity within the MPE droplets, suggesting a possible step towards controlling the chemical reactivity between different members of a protocell community comprising interacting colloidal objects.

From a general perspective our observations highlight a pathway to synthetic protocell consortia exhibiting unusual collective behaviour, and offer an opportunity to engineer mixed populations of micro-compartmentalized colloidal objects as functional microscale systems.[26] Extending current studies towards a paradigm that embraces the behaviour of artificial protocell communities as well as their individuated functionality should offer new directions for the development of synthetic protocell ecosystems based on interacting networks of micro-compartmentalized colloidal objects. In this context, biological behaviours such as phagocytosis, signalling, cooperation, specialization, endosymbiosis, predation and swarming could play a key role in inspiring the engineering of new synthetic material micro-systems with life-like properties. In particular, the introduction of artificial phagocytosis-like behavior in existing technologies involving biological material transport, biological or multi-stage catalysis, or complex bioassays could enable new colloid capture-dependent capabilities. For example, we speculate that controlled engulfment in mixed populations of synthetic protocells could have tangible advantages in microfluidic technologies involving two-phase droplet micro-reactors. These systems are restricted in their droplet chemistry by the difficulty of controlling reagent addition to an existing droplet stream such that the reactants are usually supplied at the onset of droplet formation.[33] In contrast, the multistep and sequential delivery of reagents into a MPE droplet micro-reactor via colloidosome intake would be achieved without the requirement for direct and multiple injection as commonly practiced in microfluidic devices. Moreover,

engulfment of intact colloidosomes into a MPE micro-reactor interior offers unique advantages compared with droplet fusion methods as the encapsulated enzymes can be delivered in the form of discrete catalytic packages without contamination of the external phase. From a longer term perspective, we speculate that the notion of artificial phagocytosis in mixed communities of micro-compartmentalized colloids could offer new strategies for the introduction and recovery of enzymes in oil-based decontamination and biotransformation reactions. For example, we envisage using lipase-containing colloidosomes to hydrolyse fats in waste frying oils to added-value products such as fatty acids and monoacylglycerols.[34] Subsequent capture of the silica micro-reactors by controlled fatty acid-mediated engulfment on addition of a population of MPE droplets could then be exploited magnetically to increase the efficiency of enzyme recovery and long term environmental management of diverse waste oil pollutants.

METHODS

Preparation of magnetic Pickering emulsion droplets. Water-in-oil magnetic Pickering emulsion (MPE) droplets were prepared as follows: 5 mg of partially hydrophobic oleate-capped magnetite particles (see Supplementary Methods) were added to 1 mL of dodecane (purity ≥ 99%, Sigma-Aldrich, USA) and sonicated for 1 min. The suspension was transferred to an Eppendorf tube and appropriate volumes (5-100 µL) of carbonate (pH = 10.2), tris(hydroxymethyl)aminomethane (pH = 8.3) or 2-(N-morpholino)ethanesulfonic acid (pH = 5.5) buffers were added. Typically, the water/dodecane volume ratio was 0.05, with a magnetite/water weight ratio of 0.1. The mixture was stirred for 15 s at 25000 rpm using an UltraTurrax T 10 homogenizer with a S10 D-7G-KS-65 dispersing tip (IKA, Germany). In some experiments, aqueous solutions of isothiocyanate tagged–dextran (molecular weight 150 kDa, Sigma-Aldrich, USA) or rhodamine-labelled bovine serum albumin, were encapsulated inside the Pickering emulsions to facilitate imaging of the magnetic droplets.

Preparation of silica colloidosomes. Silica colloidosomes were prepared as previously reported.[6] Briefly, 15 mg of hydrophobic silica nanoparticles (Wacker-Chemie, Germany) were dispersed in 2 mL of dodecane prior to the addition of 100 µL of an aqueous phase (typically pH ≈ 6). The mixture was then stirred using an UltraTurrax T18 homogenizer (IKA, Germany) for 30 s at 10000 rpm. A range of solutes (see below) were encapsulated within the silica colloidosomes to evaluate their delivery and release during engulfment. Crosslinking of the silica membrane in dodecane was achieved by addition of 25 µL of tetramethoxysilane (TMOS, 98%, Sigma-Aldrich, USA), after which the colloidosomes were stirred in a rotator at room temperature overnight.

Oleic acid-mediated opening of MPE droplets. Magnetic particle-stabilized water-in-dodecane droplets (pH 5.5, 8.3, 10.2) were pipetted from an Eppendorf tube and added to a polystyrene Petri dish (3.5 cm diameter, Corning, USA) filled with 1 mL of an oleic acid/dodecane solution (0.25-40 mg mL^{-1}). Fifteen optical microscopy images of different droplets were recorded after *ca.* 10-20 s for each oleic acid concentration and the images were analysed with the free software *ImageJ* to estimate differences in the percentage coverage of the magnetite particles in the membrane of the MPE droplets as a function of oleic acid concentration. For this, the shell apertures (*i.e.*, fatty-acid stabilized patches) were selected and the area of these sub-regions calculated with the software measure tool. To minimize the inaccuracy associated with the analysis of droplets viewed in 2-D optical projections in which the effects of droplet

curvature on the surface area could not be taken directly into account, the data was plotted as the percentage of the droplet area uncoated by the magnetite particles. By presenting the data as the quotient of the measured aperture area and area of the whole droplet, we sought to minimise the errors as both area measurements were associated with similar levels of inaccuracy.

Primitive artificial phagocytosis. Engulfment of water-filled silica colloidosomes in oil by MPE droplets was undertaken as follows**.** A dodecane suspension of cross-linked silica colloidosomes (200 μL, water/dodecane volume ratio = 0.05, silica/water weight ratio = 0.10-0.15, 25 μL TMOS) was mixed at room temperature with 1 mL of oleic acid in dodecane at a range of concentrations (0.25-40 mg mL^{-1}), followed by addition of 20 μL of a water-in-dodecane magnetite Pickering emulsion (water/dodecane = 0.05, magnetite/water weight ratio = 0.1, pH = 5.5, 8.3, 10.2). In some experiments, a desired number of MPE droplets (typically one or two) were pipetted into the silica colloidosome suspension. The mixtures were investigated immediately by optical and fluorescence microscopy and movies of the phagocytosis-like behaviour recorded using an Olympus BX53 microscope (Olympus, Japan) and a Leica DMI3000 B microscope (Leica, Germany), respectively.

Remote manipulation of the MPE droplets was achieved in the chamber of the optical microscope by using a neodymium cylindrical magnet (length = 6 mm, diameter = 5 mm; RS Components, UK). The magnet was attached to a thin spatula (length = 10 cm) to facilitate manual manipulation of the MPE droplets by generating localized changes in the magnetic field gradient around the sample holder. MPE droplets were attracted to areas enriched with silica colloidosomes by holding the magnet in close proximity to the silica microcapsules and following the trajectories in the optical microscope. Magnetically induced localized opening of the iron oxide shell of the MPE droplets in the presence of low oleic acid concentrations (typically ≤ 1 mg mL^{-1}) was achieved by positioning the magnet close to the side of the droplet opposite to the area where the aperture was to be produced. As a consequence, the magnetite particles moved around the surface of the emulsion droplet towards the region of higher field strength, leaving the opposite side free of inorganic nanoparticles and stabilized by a continuous oleate monolayer. In general, the magnet was positioned at an appropriate distance from the samples such that displacement of the MPE droplets from the field of view was minimized. Similar experiments were also undertaken with MPE droplets but in the presence of non-crosslinked silica nanoparticle-stabilized water-in-oil droplets in place of the cross-linked silica colloidosomes (see Supplementary Methods).

The influence of oleic acid concentration and deprotonation on colloidosome ingestion was investigated by preparing mixtures of MPE droplets produced at pH 10.2 (oleate), 8.3 (oleate/oleic acid) and 5.5 (oleic acid) and cross-linked silica colloidosomes containing carmine/curcumin red food dye (80 vol% glycerol/water) in dodecane containing oleic acid at a range of concentrations (0.25-40 mg mL^{-1}). The number of silica colloidosomes incarcerated into the MPE droplets within a period of 60 s was counted using an optical microscope and compared to the initial number of silica colloidosomes in the field of view to quantify the engulfment efficiency. This procedure was repeated for five different MPE droplets for three freshly prepared samples of cross-linked silica colloidosomes. The effect of the oleic acid concentration in the dodecane continuous phase on intake efficiency was evaluated following the same methodology for each of the assayed pHs. Similar experiments were undertaken to assess the engulfment associated with changes in the dodecane/water interfacial tension ($\gamma_{o/w}$) at a fixed oleic acid concentration of 2 mg mL^{-1} by using cross-linked silica colloidosomes

containing an aqueous solution of NaCl (0.1 M, $\gamma_{o/w}$ = 49 ± 2 mN m^{-1}), carmine/curcumin red food dye (80 vol% glycerol/water; $\gamma_{o/w}$ = 6.1 ± 1.5 mN m^{-1}) or a 25 vol% dilution of the dye ($\gamma_{o/w}$ = 11.8 ± 0.9 mN m^{-1}). In each case, the experiments were conducted in the presence or absence of an external magnetic field, and five different MPE droplets associated with six freshly prepared samples of cross-linked silica colloidosomes were analyzed. The statistical *t*-test was used to determine statistical significance (*p* values < 0.05).

Delivery and release of colloidosome-entrapped payloads. Engulfment-mediated delivery and release of molecules into the MPE droplets was investigated by encapsulating aqueous solutions of calcein (1 mg mL^{-1}, molecular radius 1.3 nm), or fluorescein isothiocyanate-tagged bovine serum albumin (5 mg $mL^{-1,}$ molecular size 14 × 4 × 4 nm) within cross-linked silica colloidosomes or non-crosslinked silica nanoparticle-stabilized water-in-oil droplets, and monitoring their release during ingestion by fluorescence microscopy. Experiments were also undertaken with non-crosslinked silica nanoparticle-stabilized water-in-oil droplets containing a 5 mg mL^{-1} suspension of green fluorescent aminated polystyrene beads (diameter = 3 μm, Corpuscular Inc., USA) in glycerol.

Engulfment-triggered dephosphorylation. 50 μL of a 1650 units mL^{-1} solution of alkaline phosphatase (ALP, CALBIOCHEM, Merck, Germany) in carbonate buffer (pH = 10.2) was encapsulated in the aqueous phase of a dispersion of MPE droplets in dodecane containing oleic acid. Non-fluorescent fluorescein diphosphate (tetra-ammonium salt, Insight Biotechnology, UK) was used as the enzyme substrate and encapsulated in the water phase (100 μL, 1 mg mL^{-1}, carbonate buffer, pH = 10.2) of a dodecane dispersion of cross-linked silica colloidosomes that was kept in the dark and at 4°C prior to addition of the ALP-containing MPE droplets. Engulfment-mediated dephosphorylation was observed by monitoring the release of fluorescein within the MPE droplets using a Leica DMI3000 B microscope (Leica, Germany) with simultaneous bright field and fluorescence imaging. The increase of fluorescence was quantified using the free software *ImageJ.* Experiments were undertaken in which engulfment of individual fluorescein diphosphate-containing colloidosomes by a single ALP-containing MPE droplet was followed by an appropriate time lapse so that changes in fluorescence intensity associated with the penetration of individual colloidosomes could be monitored without interference.

References

1. Tu, Y. *et al.* Mimicking the cell: bio-inspired functions of supramolecular assemblies. *Chem. Rev.* **116,** 2023-2078 (2016).
2. Li, M., Huang, X., Tang, T.-Y. D. & Mann, S. Synthetic cellularity based on non-lipid micro-compartments and protocell models. *Curr. Opin. Chem. Biol.* **22,** 1-11 (2014).
3. Schoonen, L. & van Hest, J. C. M. Compartmentalization approaches in soft matter science: from nanoreactor development to organelle mimics. *Adv. Mater.* **28,** 1109–1128 (2015).
4. Kelly, B. T., Baret, J. C., Taly, V. & Griffiths, A. D. Miniaturizing chemistry and biology in microdroplets. *Chem.Commun.* 1773-1788 (2007).
5. Mann, S. The origins of life: old problems, new chemistries. *Angew. Chem. Int. Ed. Engl.* **52,** 155-162 (2013).
6. Li, M., Green, D. C., Anderson, J. L. R., Binks, B. P. & Mann, S. In vitro gene expression and enzyme catalysis in bio-inorganic protocells. *Chem. Sci.* **2,** 1739-1745 (2011).
7. Li, M., Huang, X. & Mann, S. Spontaneous growth and division in self-reproducing inorganic colloidosomes. *Small* **10,** 3291–3298 (2014).
8. Li, M., Harbron, R. L., Weaver, J. V. M., Binks, B. P. & Mann, S. Electrostatically gated membrane permeability in inorganic protocells. *Nat. Chem.* **5,** 529–536 (2013).
9. Pagonabarraga, I. Wetting dynamics: adsorbed colloids relax slowly. *Nat. Mater.* **11,** 99–100 (2012).
10. Tang, J., Quinlan, P. J. & Tam, K. C. Stimuli-responsive Pickering emulsions: recent advances and potential applications. *Soft Matter* **11,** 3512–3529 (2015).
11. Dinsmore, D. *et al.* Colloidosomes: selectively permeable capsules composed of colloidal particles. *Science* **298,** 1006–1009 (2002).
12. Li, Y. *et al.* Magnetic hydrogels and their potential biomedical applications. *Adv. Funct. Mater.* **23,** 660–672 (2013).
13. Wu, C., Bai, S., Ansorge-Schumacher, M. B. & Wang, D. Nanoparticle cages for enzyme catalysis in organic media. *Adv. Mater.* **23,** 5694–5699 (2011).
14. Akkarachaneeyakorn, K., Li, M., Davis, S. A. & Mann, S. Secretion and reversible assembly of extracellular-like matrix by enzyme-active colloidosome-based protocells. *Langmuir* **32,** 2912–2919 (2016).
15. Sun, S. *et al.* Chemical signalling and functional activation in colloidosome-based protocells. *Small* **12,** 1920–1927 (2016).
16. Nourian, Z. & Danelon, C. Linking genotype and phenotype in protein synthesizing liposomes with external supply of resources. *ACS Synth. Biol.* **2,** 186-193 (2013).
17. Martini, L. & Mansy, S. S. Cell-like systems with riboswitch controlled gene expression. *Chem. Commun.* **47,** 10734-10736 (2011).
18. Peters, R. J. R. W. *et al.* Cascade reactions in multicompartmentalized polymersomes. *Angew. Chem. Int. Ed.* **53,** 146-150 (2014).
19. Chandrawati, R. & Caruso, F. Biomimetic liposome- and polymersome-based multicompartmentalized assemblies. *Langmuir* **28,** 13798-13807 (2012).
20. Tawfik, D. S. & Griffiths, A. D. Man-made cell-like compartments for molecular evolution. *Nat. Biotechn.* **16**, 652-656 (1998).
21. Huang, X., Patil, A. J., Li, M. & Mann, S. Design and construction of higher-order structure and function in proteinosome-based protocells. *J. Am. Chem. Soc.* **136,** 9225-9234 (2014).
22. Huang, X., *et al.* Interfacial assembly of protein-polymer nano-conjugates into stimulus-responsive biomimetic protocells. *Nat. Commun.* **4,** 2239 (2013).
23. Koga, S., Williams, D. S., Perriman, A. W. & Mann, S. Peptide-nucleotide microdroplets as a step towards a membrane-free protocell model. *Nat. Chem.* **3,** 720-724 (2011).
24. Tang, T.-Y. D. *et al.* Fatty acid membrane assembly on coacervate microdroplets as a step towards a hybrid protocell model. *Nat. Chem.* **6,** 527-533 (2014).
25. Rollie, S., Mangold, M. & Sundmacher, K. Designing biological systems: systems engineering meets synthetic biology. *Chem. Eng. Sci.* **69,** 1-29 (2012).
26. Qiao, Y., Li, M., Booth. R. & Mann, S. Predatory behaviour in synthetic protocell communities. *Nat. Chem.* **9,** 110-119 (2017).
27. Schwarz-Schilling, M., Aufinger, L., Muckl, A. & Simmel, F. C. Chemical communication between bacteria and cell-free gene expression systems within linear chains of emulsion droplets. *Integr. Biol.* **8,** 564-570 (2016).
28. Weitz, M. *et al.* Diversity in the dynamical behaviour of a compartmentalized programmable biochemical oscillator. *Nat. Chem.* **6,** 295–302 (2014).

29. Bekki, S., Vignes-Adler, M., Nakache, E. & Adler, P. M. Solutal Marangoni effect. *J. Colloid. Inter. Sci.* **140,** 492-506 (1990).
30. Toyota, T., Maru, N., Hanczyc, M.M., Ikegami, T. & Sugawara, T. Self-Propelled Oil Droplets Consuming "Fuel" Surfactant. *J. Am. Chem. Soc.* **131**, 5012-5013 (2009).
31. Hanczyc, M. M., Toyota, T., Ikegami, T., Packard, N. & Sugawara, T. Fatty acid chemistry at the oil−water interface: self-propelled oil droplets. *J. Am. Chem. Soc.* **129,** 9386-9391 (2007).
32. Ban T., Yamagami, T., Nakata, H. & Okano, Y. pH-dependent motion of self-propelled droplets due to Marangoni effect at neutral pH. *Langmuir* **29,** 2554-2561 (2013).
33. Nightingale, A. M., Phillips, T. W., Bannock, J. H. & de Mello, J. C. Controlled multistep synthesis in a three-phase droplet reactor. *Nat. Commun.* **5**: 3777 (2014).
34. Moya-Ramírez, I., García-Román, M. & Fernández-Arteaga, A. Waste frying oil hydrolysis in a reverse micellar system. *ACS Sustainable Chem. Eng*., **4,** 1025-1031 (2016).

Acknowledgements
We thank the European Union's Horizon 2020 research and innovation programme for funding the work under Marie Skłodowska-Curie grant agreement, No. 656490, Dr Avinash Patil for fruitful discussions, Ms Laura Powell for help with magnetite particle synthesis and MPE droplet preparation, and the Krüss Facility and Electron Microscopy Unit (School of Chemistry, University of Bristol) for assistance with, contact angle/interfacial tension measurements and SEM imaging, respectively.

Author contributions
LR-A, ML, SM conceived the experiments; LR-A performed the experiments; LR-A and ML undertook the data analysis; LR-A, ML, SM wrote the manuscript.

Additional information
Supplementary information is available in the online version of the paper. Reprints and permissions information is available online at www.nature.com/reprints. Correspondence and requests for materials should be addressed to S.M.

Competing financial interests
The authors declare no competing financial interests.

Data availability statement
The authors declare that all relevant data supporting the finding of this study are available within the paper and its Supplementary Information files. Additional data are available from the corresponding author upon request.

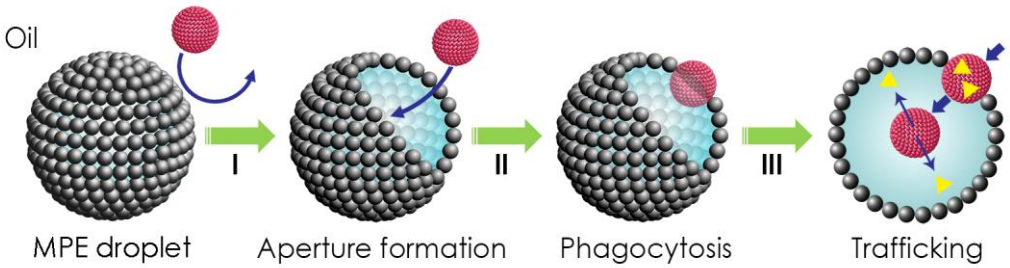

Figure 1. Design concept for phagocytosis-inspired behaviour. Scheme showing overall strategy for the spontaneous ingestion of cross-linked water-filled silica colloidosomes (red objects) by larger water-in-oil magnetic Pickering emulsion (MPE) droplets in an oil continuous phase. Addition of oleic acid to the oil phase (**I**) results in aperture formation in the MPE droplets. As a consequence, the initially non-interacting micro-compartmentalized colloidal objects become susceptible to a rudimentary process of artificial phagocytosis without disruption of either the silica or iron oxide microcapsules (**II**). Molecular encapsulation within the silica colloidosomes (**III**) results in trafficking and triggered release of the payloads (small triangles).

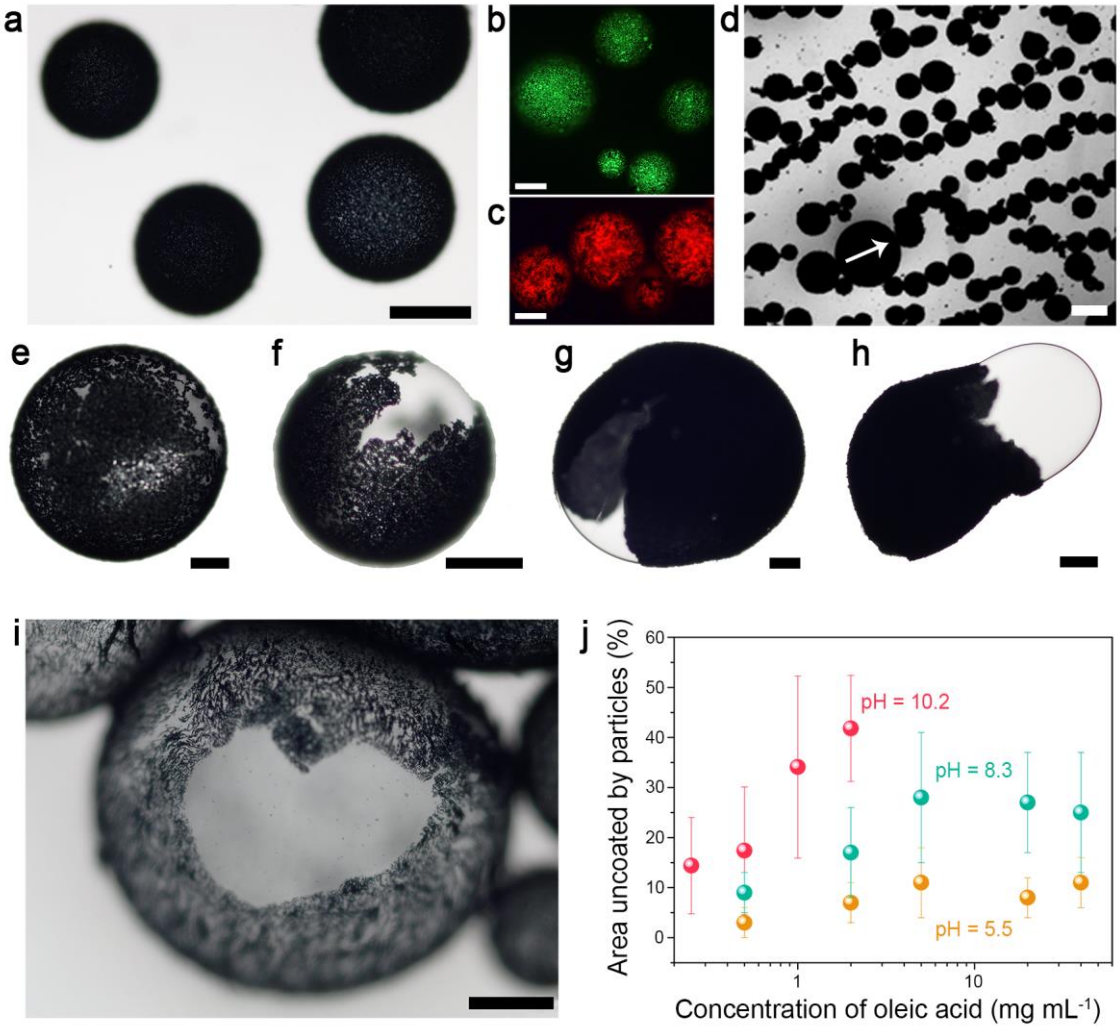

Figure 2. Aperture formation in MPE droplets. a, Optical microscopy image showing spherical MPE droplets dispersed in dodecane. The droplets are stabilised by a monolayer shell of closely packed magnetic particles and appear as optically dense micro-compartmentalized colloidal objects; scale bar = 200 µm. **b,c**, Fluorescence microscopy images of MPE droplets containing encapsulated fluorescein isothiocyanate tagged-dextran (green) (**b**), or rhodamine-labelled bovine serum albumin (red) (**c**); scale bars = 200 µm. **d,** Optical microscopy image showing linear arrays of MPE droplets aligned along the magnetic field direction (arrow) of an externally placed neodymium magnet. Scale bar = 200 µm. **e-h,** Optical microscopy images showing structural and morphological differences in MPE droplets prepared at pH 10.2 and oleic acid concentrations of 0.25 (**e**), 0.5 (**f**), 1.0 (**g**) and 2.0 mg mL^{-1} (**h**); scale bars = 100 µm. **i,** Optical microscope image showing a large fatty-acid stabilized aperture associated with the magnetite shell of a single MPE droplet (pH = 10.2, oleic acid = 2.0 mg mL^{-1}; scale bar = 100 µm. **j,** Plot showing percentage of MPE droplet surface area associated with aperture formation (% uncoated by magnetic particles) as a function of oleic acid concentration in the oil and pH of the droplets. MPE droplets prepared at pH 5.5 (MES buffer) were structurally and morphologically unaffected by the addition of oleic acid even at concentrations as high as 40 mg mL^{-1}. Data obtained from optical microscopy images. Bars on data points represent standard deviations.

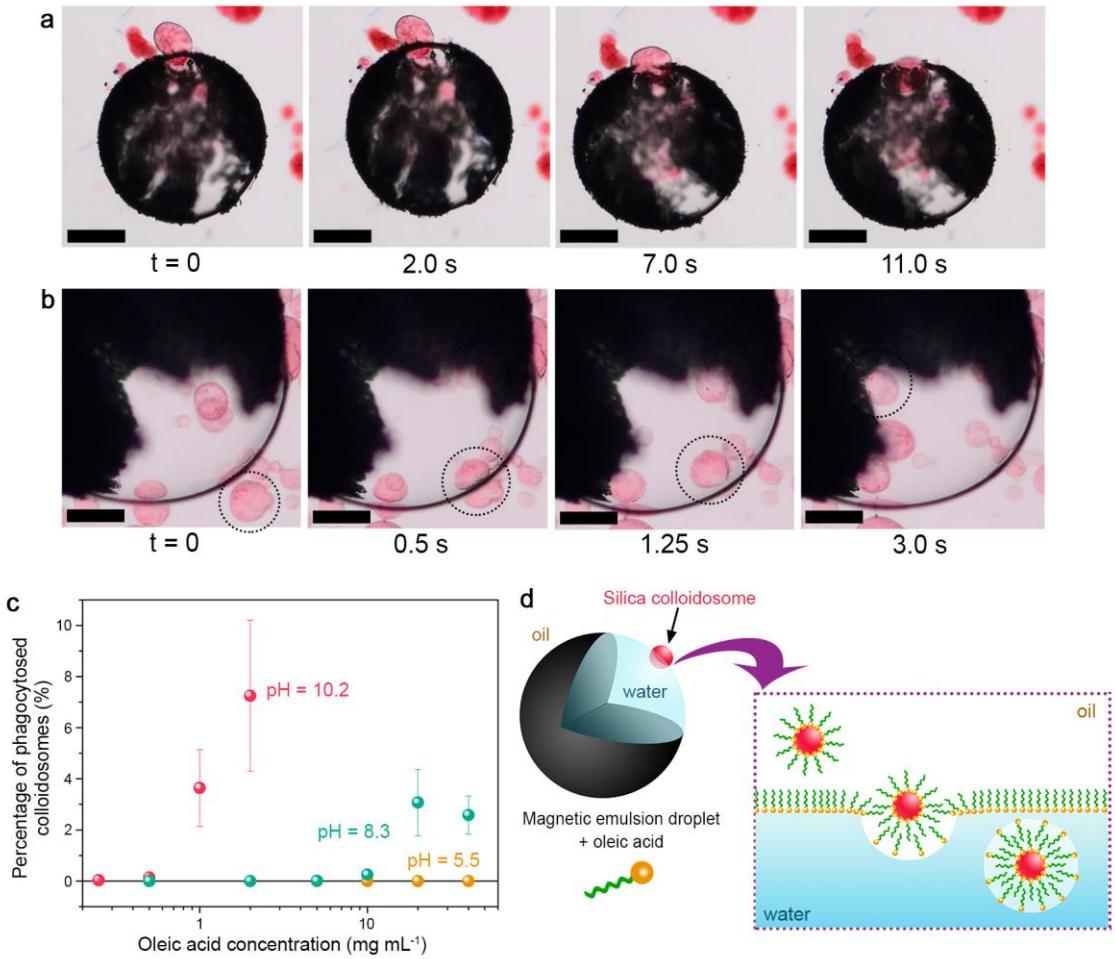

Figure 3. Engulfment of silica colloidosomes by MPE droplets. **a,** Time sequence of optical microscopy images showing attachment of a dye (carmine)-loaded cross-linked colloidosome (red object) to the surface of an individual MPE droplet (pH 10.2) dispersed in dodecane containing 1 mg mL^{-1} oleic acid, followed by magnetically induced opening of the magnetite shell and slow ingestion of the colloidosome through the aperture. Scale bar = 100 µm. See Supplementary Movie 1 for complete sequence. **b,** Time sequence of optical microscopy images showing spontaneous transfer of a dye-loaded cross-linked silica colloidosome (red object, dotted line) into a MPE droplet (pH 10.2, oleic acid = 2 mg mL^{-1}). Penetration of the intact colloidosome occurs at the magnetite-free aperture with a transit time of a few seconds. Phagocytosis-like behaviour occurs in both the presence and absence of the magnetic field. Scale bar = 100 µm. **c,** Plot showing percentage of silica colloidosomes ingested by MPE droplets ("phagocytosed colloidosomes") after 60 s with respect to the total number of colloidosomes in the field of view of the optical microscope as a function of oleic acid concentration and droplet pH. No magnetic field was applied. Error bars correspond to standard deviations. **d,** Proposed mechanism for primitive artificial phagocytosis. Translocation of intact colloidosomes is facilitated by the reduced interfacial tension of the oleate-stabilized patches on the MPE membrane (left image) as well as *in situ* assembly of a fatty acid bilayer or multilayer on the external surface of the colloidosome during transfer across the interface (right image).

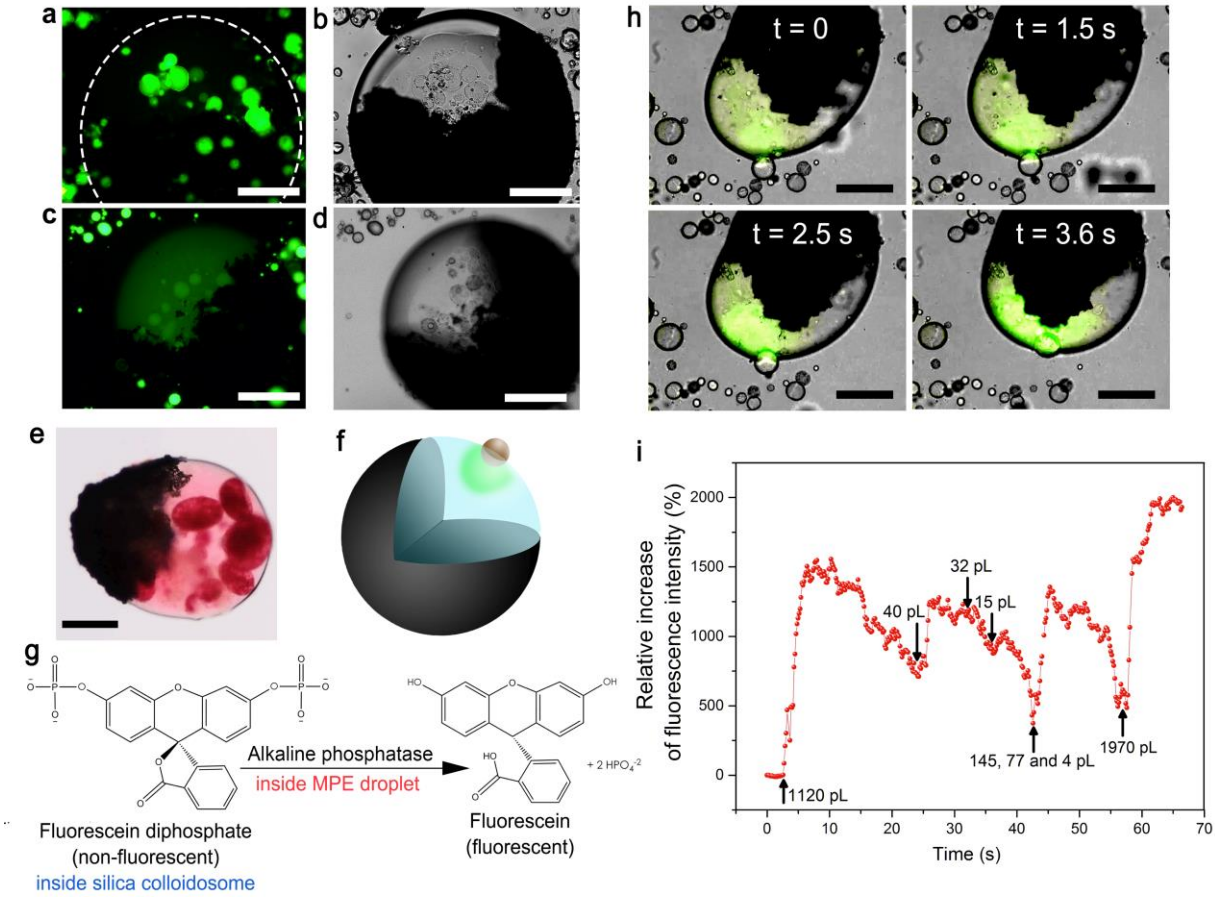

Figure 4. Payload delivery, release and reactivity. **a,b,** Fluorescence (**a**) and corresponding bright field (**b**) images of a single MPE droplet (pH 10.2; oleic acid = 2 mg mL^{-1}) after ingestion of several silica colloidosomes containing FITC-BSA. Green fluorescence is associated only with the engulfed colloidosomes indicating that the protein is not released into the interior of the MPE droplet. The fluorescence intensities of the ingested and non-engulfed colloidosomes are the same; scale bar = 200 µm. Dashed line in (**a**) delineates the position of the MPE droplet boundary. **c,d,** Fluorescence (**c**) and corresponding bright field (**d**) images of a single MPE droplet (pH 10.2; oleic acid = 2 mg mL^{-1}) recorded after intake of several calcein-containing silica colloidosomes. Green fluorescence is observed both within the ingested colloidosomes and aqueous phase of the MPE droplet due to leakage of the payload through the silica membrane. The fluorescence intensity of the ingested colloidosomes is considerably lower than for colloidosomes dispersed in the surrounding oil phase; scale bar = 200 µm. **e,** Optical microscope image of a single MPE droplet (pH 10.2; oleic acid = 2 mg mL^{-1}) showing engulfed colloidosomes containing the red dye, carmine. The pink-colouration is due to leakage of the dye after ingestion into the aqueous interior of the MPE droplet; scale bar = 200 µm. **f,g,** Enzyme catalysis in MPE droplets: **(f)** sketch illustrating basic design; silica colloidosome (brown) with an encapsulated pro-fluorescent substrate (fluorescein diphosphate, pH = 10, 1 mg mL^{-1}) is engulfed through an oleate-stabilized aperture of an ALP-containing MPE droplet (pH 10.2, oleic acid = 2 mg mL^{-1}) followed by release of the payload and reaction with the enzyme to produce a fluorescent product (green); (**g**) ALP-mediated dephosphorylation of fluorescein diphosphate produces fluorescein inside the MPE droplets, which enables phagocytosis and enzyme activity to be monitored by bright field imaging and fluorescence microscopy ($\lambda_{emission}$ = 521 nm). **h,** Time sequence of fluorescence microscopy images showing penetration of a non-fluorescent fluorescein diphosphate-containing silica colloidosome across the entry point of a MPE droplet (pH 10.2; oleic acid = 2 mg mL^{-1}) containing ALP. Contact with the aqueous phase of the MPE droplet gives rise to green fluorescence as the substrate is released and reaction with ALP occurs. The fluorescence intensity increases as the silica colloidosome penetrates further into the MPE droplet; scale bar = 200 µm. **i,** Plot showing relative increase in fluorescence intensity with time for six episodic colloidosome ingestion events involving a single MPE droplet (see Supplementary Movie 9). Arrows indicate the onset of engulfment and subsequent increases in green fluorescence; associated lettering give the estimated volumes of each ingested colloidosome. Single colloidosomes are engulfed except for event 5, which comprises the simultaneous ingestion of three colloidal objects. The decrease in fluorescence intensity after each engulfment is associated with local dilution of the fluorescein product due to turbulence inside the MPE droplet.